The classical limit for a class of quantum baker's maps

2002 J. Phys. A: Math. Gen. 35 8341

(http://iopscience.iop.org/0305-4470/35/39/314)

INSTITUTE OF PHYSICS PUBLISHING JOURNAL OF PHYSICS A: MATHEMATICAL AND GENERAL

J. Phys. A: Math. Gen. **35** (2002) 8341–8360 PII: S0305-4470(02)37781-3

The classical limit for a class of quantum baker's maps

Mark M Tracy and A J Scott

Department of Physics and Astronomy, University of New Mexico, Albuquerque, NM 87131-1156, USA

E-mail: mtracy@phys.unm.edu and ascott@phys.unm.edu

Received 7 June 2002
Published 17 September 2002
Online at stacks.iop.org/JPhysA/35/8341

Abstract

We show that the class of quantum baker's maps defined by Schack and Caves have the proper classical limit provided the number of momentum bits approaches infinity. This is done by deriving a semi-classical approximation to the coherent-state propagator.

PACS numbers: 05.45.Mt, 03.65.Sq

1. Introduction

The introduction of 'toy' mappings which demonstrate essential features of nonlinear dynamics has led to many insights in the field of classical chaos. A well-known example is the so-called *baker's transformation* [1]. Interest in this mapping stems from its straightforward characterization in terms of a Bernoulli shift on binary sequences. It seems natural to consider a quantum counterpart to the baker's map for the investigation of quantum chaos. Unfortunately, there is no unique quantization procedure, and hence we must embrace the possibility of different quantum maps limiting to the same classical baker's transformation.

Balazs and Voros [2] were first to conceive a quantum version of the baker's map. This was done with the help of the discrete quantum Fourier transform. Subsequently, improvements to the Balazs–Voros quantization were made by Saraceno [3], an optical analogy was found [4], a canonical quantization was devised [5, 6], and quantum computing realizations have been proposed [7, 8]. A quantum baker's mapping on the sphere has also been defined [9]. More recently, an entire class of quantum baker's maps was proposed by Schack and Caves using qubits [10]. The Balazs–Voros quantization is but one member of this class.

The classical limit of the Schack–Caves quantizations is the subject of this paper. We explicitly derive a semi-classical approximation for the propagator in the coherent state basis. This enables us to give conditions upon which the Schack–Caves quantizations will behave as the classical baker's transformation in the limit $\hbar \to 0$. We find that, provided the number of

momentum qubits approaches infinity, the semi-classical propagator takes the form

$$\langle b|\hat{B}|a\rangle \approx \sqrt{\frac{\partial^2 W}{\partial a \partial b^*}} \exp[W(b^*, a)/2\hbar] \exp[-(|a|^2 + |b|^2)/4\hbar]$$

where $|a\rangle$ and $|b\rangle$ are coherent states on the torus, and $W(b^*, a)$ is a classical generating function. Similar propagators have been encountered before using spin coherent states [11, 12], but all may be thought of as variants of those derived long ago by Van Vleck [13] and Gutzwiller [14]. Semi-classical propagators play an important role in the path-integral formulation of quantum mechanics [15] and the related theory of periodic orbit quantization [16]. The latter has been investigated thoroughly for the Balazs–Voros quantum baker's map [17–25].

In deriving a semi-classical approximation only for the one-step propagator, we avoid complications which will arise after many iterations of the mapping. For long time scales, simple quantum-to-classical correspondences will break down [26] and one must incorporate the theories of decoherence [27–29] or continuous measurement [30, 31]. The classical limit of the Schack–Caves quantization has already been investigated [32] in this light using a decoherent histories approach [33–35]. However only a special case ($\theta = 0$ in our notation) was considered. We proceed under an assumption that provided our one-step propagator agrees with the baker's transformation in the semi-classical limit $\hbar \to 0$, decoherence will restore quantum-to-classical correspondences for long time scales.

The paper is organized as follows. In section 2, we introduce the baker's map, both in classical and quantal form. Coherent states for a toroidal phase space are also introduced. In section 3 our core results are presented. Here we derive semi-classical approximations to the coherent-state propagator and give conditions for when the Schack–Caves quantizations have the proper classical limit. Finally, in section 4, we summarize our findings.

2. A class of quantum baker's maps

The baker's map is a standard example in chaotic dynamics. It is a mapping of the unit square onto itself in the form

$$q_{n+1} = 2q_n - \lfloor 2q_n \rfloor \tag{1}$$

$$p_{n+1} = (p_n + \lfloor 2q_n \rfloor)/2 \tag{2}$$

where $q, p \in [0, 1)$, $\lfloor x \rfloor$ is the integer part of x, and n denotes the nth iteration of the map. Geometrically, the map stretches the unit square by a factor of 2 in the q direction, squeezes by a factor of a half in the p direction, and then stacks the right half onto the left.

The map's action may be rewritten in terms of the complex variable $a \equiv q + \mathrm{i}p$,

$$a_{n+1} = \frac{5}{4}a_n + \frac{3}{4}a_n^* + \left(\frac{\mathrm{i}}{2} - 1\right) \lfloor a_n + a_n^* \rfloor \equiv b_n(a_n, a_n^*). \tag{3}$$

A generating function for this mapping (up to an arbitrary constant) is

$$W(b^*, a) = \frac{1}{10}(3b^{*2} + 8ab^* - 3a^2) + \frac{4}{5}\left(1 + \frac{\mathrm{i}}{2}\right)\left(a + \mathrm{i}b^* - \frac{1}{2}\right) \lfloor a + a^* \rfloor \tag{4}$$

assuming $a + a^*$ non-integer. The classical baker's map may then be rederived *via* the relations

$$\frac{\partial W}{\partial b^*} = b \qquad \frac{\partial W}{\partial a} = a^*. \tag{5}$$

Interest in the baker's map is due mainly to the simplicity of its *symbolic dynamics*. If each point of the unit square is identified through its binary representation, $q = 0 \cdot s_1 s_2 \ldots =$

$\sum_{k=1}^{\infty} s_k 2^{-k}$ and $p = 0 \cdot s_0 s_{-1} \ldots = \sum_{k=0}^{\infty} s_{-k} 2^{-k-1}$ ($s_i \in \{0, 1\}$), with a bi-infinite symbolic string

$$s = \ldots s_{-2} s_{-1} s_0 \bullet s_1 s_2 s_3 \ldots \tag{6}$$

then the action of the baker's map is to shift the position of the dot by one point to the right,

$$s \to s' = \ldots s_{-2} s_{-1} s_0 s_1 \bullet s_2 s_3 \ldots . \tag{7}$$

For a quantum mechanical version of the map, we work in the D-dimensional Hilbert space, $\mathcal{H}_D$, spanned by either the position states $|q_j\rangle$, with eigenvalues $q_j = (j + \beta)/D$, or momentum states $|p_k\rangle$, with eigenvalues $p_k = (k+\alpha)/D$ ($j, k = 0, \ldots, D-1$). The constants $\alpha, \beta \in [0, 1)$ determine the periodicity of the space: $|q_{j+D}\rangle = \mathrm{e}^{-2\pi \mathrm{i}\alpha}|q_j\rangle$, $|p_{k+D}\rangle = \mathrm{e}^{2\pi \mathrm{i}\beta}|p_k\rangle$. Such double periodicity identifies $\mathcal{H}_D$ with a toroidal phase space. The vectors of each basis are orthonormal $\langle q_j|q_{j'}\rangle = \delta_{j,j'}$, $\langle p_k|p_{k'}\rangle = \delta_{k,k'}$ and the two bases are related via the finite Fourier transform

$$\langle q_j|\hat{F}_D|q_k\rangle \equiv \langle q_j|p_k\rangle = \frac{1}{\sqrt{D}}\,\mathrm{e}^{\frac{\mathrm{i}}{\hbar} q_j p_k}.$$

For consistency of units, we must have $2\pi\hbar D = 1$.

The first work on a quantum baker's map was done by Balazs and Voros [2]. Their expression for the map was given in the form

$$\hat{B} = \hat{F}_D^{-1} \begin{pmatrix} \hat{F}_{D/2} & 0 \\ 0 & \hat{F}_{D/2} \end{pmatrix} \tag{8}$$

where $\hat{F}_{D/2}$ is the finite Fourier transform acting on half of the Hilbert space. Later, Saraceno [3] improved certain symmetry characteristics of the map using anti-periodic boundary conditions $\left(\alpha = \beta = \frac{1}{2}\right)$. Finally, taking again the anti-periodic Hilbert space, Schack and Caves [10] introduced a whole class of quantum baker's maps for dimensions $D = 2^N$.

For these cases, we can model our space as the product of N qubits with a binary expansion association

$$|q_j\rangle = |x_1\rangle \otimes |x_2\rangle \otimes \cdots \otimes |x_N\rangle \qquad x_l \in \{0, 1\} \tag{9}$$

where j has the binary expansion

$$j = x_1 \ldots x_N \cdot 0 = \sum_{l=1}^{N} x_l 2^{N-l} \quad \text{and} \quad q_j = \frac{j + 1/2}{D}. \tag{10}$$

Next, we rewrite the quantum Fourier transform as

$$|p_k\rangle = \hat{F}_D|q_k\rangle = \frac{1}{\sqrt{2^N}} \sum_{x_1,\ldots,x_N} |x_1\rangle \otimes |x_2\rangle \otimes \cdots \otimes |x_N\rangle\, \mathrm{e}^{2\pi \mathrm{i} y x/2^N} \tag{11}$$

where $y = y_1 \ldots y_N \cdot 1 = k + \frac{1}{2}$ and $x = x_1 \ldots x_N \cdot 1 = j + \frac{1}{2}$.

The connection with the classical baker's map comes from its symbolic dynamics. In the quantum case, a string is created through the partial Fourier transform $\hat{G}_n$. It is an operator which Fourier transforms the $N - n$ least significant qubits of a state

$$\begin{aligned} &\hat{G}_n(|x_1\rangle \otimes \cdots \otimes |x_n\rangle \otimes |a_1\rangle \otimes \cdots \otimes |a_{N-n}\rangle) \\ &\qquad \equiv |x_1\rangle \otimes \cdots \otimes |x_n\rangle \otimes \frac{1}{\sqrt{2^{N-n}}} \sum_{x_{n+1},\ldots,x_N} |x_{n+1}\rangle \otimes \cdots \otimes |x_N\rangle\, \mathrm{e}^{2\pi \mathrm{i} a x/2^{N-n}} \end{aligned} \tag{12}$$

where a and x are defined through the binary expansions $a = a_1 \ldots a_{N-n} \cdot 1$ and $x = x_{n+1} \ldots x_N \cdot 1$. In the limiting cases, we have $\hat{G}_0 = \hat{F}_D$ and $\hat{G}_N = \mathrm{i}\hat{1}$.

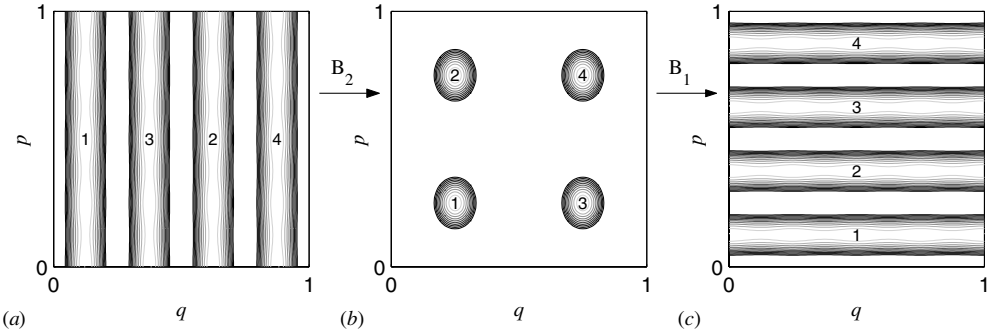

Figure 1. The Husimi function for each partially Fourier transformed state (13) when $N = 2$, and (*a*) $n = 2$, (*b*) $n = 1$ and (*c*) $n = 0$.

The analogy to the classical case is made clear through the definition

$$|a_{N-n} \dots a_1 \bullet x_1 \dots x_n\rangle \equiv \hat{G}_n(|x_1\rangle \otimes \cdots \otimes |x_n\rangle \otimes |a_1\rangle \otimes \cdots \otimes |a_{N-n}\rangle). \tag{13}$$

These states form an orthonormal basis and are localized in both position and momentum. They are strictly localized in a position region of width $1/2^n$ centred at $0 \cdot x_1 \dots x_n 1$, and are roughly localized in a momentum region of width $1/2^{N-n}$ centred at $0 \cdot a_1 \dots a_{N-n} 1$.

Using this notation, Schack and Caves defined a whole class of quantum baker's maps $\hat{B}_n$ $(n = 1, \dots, N)$:

$$\hat{B}_n \equiv \hat{G}_{n-1} \circ \hat{G}_n^{-1} = \sum_{\substack{x_1,\dots,x_n \\ a_1,\dots,a_{N-n}}} |a_{N-n} \dots a_1 x_1 \bullet x_2 \dots x_n\rangle\langle a_{N-n} \dots a_1 \bullet x_1 x_2 \dots x_n|. \tag{14}$$

The Balazs–Voros–Saraceno quantum baker's map is recovered when $n = 1$. In the language of equation (6), we see that each quantum baker's map takes a state localized at $1a_{N-n} \dots a_1 \bullet x_1 \dots x_n 1$ to a state localized at $1a_{N-n} \dots a_1 x_1 \bullet x_2 \dots x_n 1$. The decrease in the number of position bits and increase in momentum bits enforces a stretching and squeezing of phase space in a manner resembling the classical baker's map. In figure 1(*a*), (*b*) and (*c*), we have plotted the Husimi function (defined below) for the partially Fourier transformed states (13) when $N = 2$, and $n = 2$, 1 and 0, respectively. The quantum baker's map is simply a one-to-one mapping of one basis to another.

It will be useful to rewrite our baker's map in the position basis. To do this, we first use (12) and (13) to rewrite equation (14) as

$$\hat{B}_n = \frac{\sqrt{2}}{2^{N-n+1}} \sum_{\substack{x_1,\dots,x_n \\ a_1,\dots,a_{N-n}}} \sum_{\substack{z_1,\dots,z_{N-n+1} \\ y_1,\dots,y_{N-n}}} |\bullet x_2 \dots x_n z_1 \dots z_{N-n+1}\rangle\langle \bullet x_1 \dots x_n y_1 \dots y_{N-n}| \times \exp\left[\frac{\pi \mathrm{i}}{2^{N-n}}\left(\left(j+\tfrac{1}{2}\right)\left(l+\tfrac{1}{2}\right) + 2^{N-n}x_1\left(l+\tfrac{1}{2}\right) - 2\left(j+\tfrac{1}{2}\right)\left(k+\tfrac{1}{2}\right)\right)\right] \tag{15}$$

where

$$j = \sum_{k=1}^{N-n} a_k 2^{N-n-k} \qquad k = \sum_{k=1}^{N-n} y_k 2^{N-n-k} \qquad \text{and} \qquad l = \sum_{k=1}^{N-n+1} z_k 2^{N-n+1-k}.$$

Next, using (9), (13) and the notation $q_j = \left(j+\frac{1}{2}\right)/D$, $q_k = \left(k+\frac{1}{2}\right)/D$ etc, we arrive at the

quantum baker's map in the position basis

$$\hat{B}_n = \frac{\sqrt{2}}{2^{N-n+1}} \sum_{x_1=0}^{1} \sum_{j,k=0}^{2^{N-n}-1} \sum_{l=0}^{2^{N-n+1}-1} \sum_{m=0}^{2^{n-1}-1} |q_l + q_m 2^{N-n+1} - 2^{-n}\rangle\langle q_k + x_1/2 + q_m 2^{N-n} - 2^{-n-1}| \exp[\mathrm{i}\pi D 2^n (q_j q_l + 2^{-n} x_1 q_l - 2 q_j q_k)]. \tag{16}$$

Note that it is possible to sum over the index j at this point. However, the above representation proves to be most convenient when performing our semi-classical analysis.

We will now introduce *coherent states* for $\mathcal{H}_D$ [36–38],

$$|a\rangle \equiv \frac{1}{\mathcal{N}} \left(\frac{2}{D}\right)^{1/4} \sum_{\mu=-\infty}^{\infty} \sum_{j=0}^{D-1} \exp\left[-\frac{\pi D}{2}(|a|^2 - a^2) - \pi D(q_j - a + \mu)^2 + \mathrm{i}\pi\mu\right] |q_j\rangle \tag{17}$$

$$= \frac{1}{\mathcal{N}} \left(\frac{2}{D}\right)^{1/4} \sum_{j=0}^{D-1} \exp\left[-\frac{\pi D}{2}(|a|^2 + a^2) - \pi D\left(q_j^2 - 2q_j a\right)\right] \theta_0[\mathrm{i}D(q_j - a)|\mathrm{i}D]|q_j\rangle \tag{18}$$

where $a \equiv q + \mathrm{i}p$ and θ_0 is called a *theta function* [39]

$$\theta_0[z|\tau] \equiv \sum_{\mu=-\infty}^{\infty} \exp[\mathrm{i}\pi(\tau\mu^2 + (2z+1)\mu)]. \tag{19}$$

The coherent states obey $|a \pm 1\rangle = -\exp[\pm\pi\mathrm{i}Dp]|a\rangle$, $|a \pm \mathrm{i}\rangle = -\exp[\mp\pi\mathrm{i}Dq]|a\rangle$, and are simply the standard (Weyl group) coherent states that have been (anti-) periodicized and then projected onto $\mathcal{H}_D$. The normalization factor takes the form

$$\mathcal{N}^2 = \theta_0[qD|\mathrm{i}D/2]\theta_0[pD|\mathrm{i}D/2] = 1 + O(1/D) \qquad (D \text{ even}) \tag{20}$$

and, henceforth, will be set to unity. Finally, the *Husimi function* for our toroidal phase space is defined as $|\langle\psi|a\rangle|^2$.

3. The semi-classical propagator

Our goal in this section is to explicitly calculate the semi-classical propagator in the coherent state basis; that is, we wish to obtain the leading term in an asymptotic expansion of the matrix element $\langle b|\hat{B}_n|a\rangle$ as $D \to \infty$. Observe from equation (14) that in this limit, the total number of position and momentum bits N necessarily becomes infinite. However, one has considerable freedom of choice on how this may occur (see figure 2). We wish to consider cases where the relative numbers of position and momentum bits approach infinity at different rates. To this end, we take the number of position bits to be in the explicit form $n = n(N) \equiv \theta N + s$, where $0 \leqslant \theta \leqslant 1$ is rational and s takes integer values. For ease of reading, we also introduce the constant $\phi = 1 - \theta$ such that the number of momentum bits $N - n = \phi N - s$. We will also now identify the different quantum baker's maps through the new parameters, $\hat{B}_{\theta,s} \equiv \hat{B}_n$. The parameter θ (ϕ) may be interpreted as the fraction of qubits allocated to the position (momentum) register as the total number of qubits N is increased. In the analysis that follows, we must consider the two cases $\theta = 0$ and $\theta = 1$ separately. The former contains the original Balazs–Voros–Saraceno quantization ($n = s = 1$) and will be investigated first. The second parameter s describes an initial offset between the numbers of position and momentum qubits and has no semi-classical effect when $\theta < 1$. We will find, however, that s becomes important when $\theta = 1$.

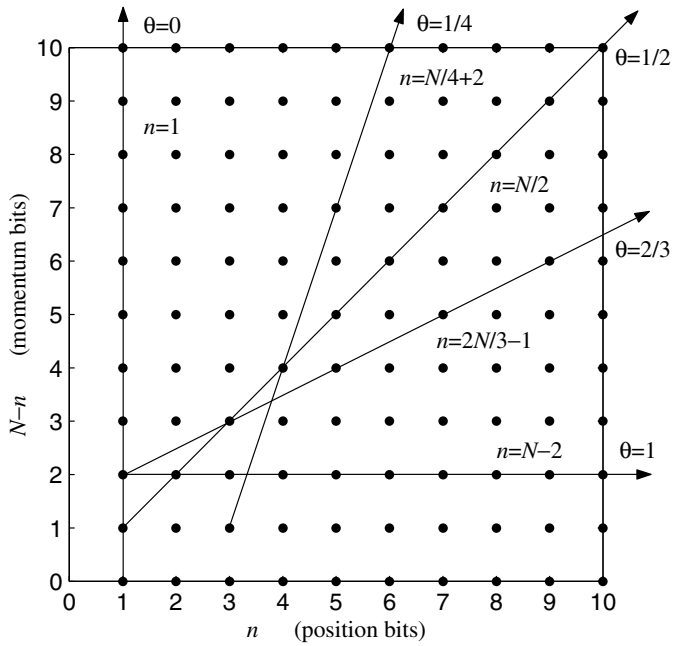

Figure 2. Different possible ways of taking the classical limit for the quantum baker's map.

3.1. Case $\theta = 0$

In this case, the number of position bits remains constant $n = s \geqslant 1$ as we let $D \to \infty$. Using (16) and (17) our matrix element becomes

$$\langle b|\hat{B}_{0,s}|a\rangle = SD^{-3/2} \sum_{\mu,\nu=-\infty}^{\infty} \sum_{x_1=0}^{1} \sum_{j,k=0}^{D/S-1} \sum_{l=0}^{2D/S-1} \sum_{m=0}^{S/2-1} \exp\Big[-\frac{\pi D}{2}(|a|^2+|b|^2-a^2-b^{*2}) + \mathrm{i}\pi(\mu-\nu) - \pi D\left(q_k + x_1/2 + \left(Dq_m - \tfrac{1}{2}\right)/S - a + \mu\right)^2 - \pi D\left(q_l + 2\left(Dq_m - \tfrac{1}{2}\right)/S - b^* + \nu\right)^2 + \mathrm{i}\pi SD(q_j q_l + x_1 q_l/S - 2q_j q_k)\Big] \tag{21}$$

where $S \equiv 2^s$. To further the calculation, we now use variants of the Poisson summation formula to replace each sum with D in the upper limit by an integral, e.g.

$$\sum_{\alpha=-\infty}^{\infty} \int_0^{1/S} \exp\left[2\pi\mathrm{i}\left(Dx - \tfrac{1}{2}\right)\alpha\right] f(x)\,\mathrm{d}x = \frac{1}{D}\int_0^{1/S} \sum_{j=-\infty}^{\infty} \delta\left(x - \left(j+\tfrac{1}{2}\right)/D\right) f(x)\,\mathrm{d}x = \frac{1}{D}\sum_{j=0}^{D/S-1} f(q_j). \tag{22}$$

The result is

$$\langle b|\hat{B}_{0,s}|a\rangle = SD^{3/2} \sum_{\substack{\mu,\nu,\alpha \\ \beta,\gamma=-\infty}}^{\infty} \sum_{x_1=0}^{1} \sum_{m=0}^{S/2-1} \int_0^{1/S} \mathrm{d}x \int_0^{1/S} \mathrm{d}y \int_0^{2/S} \mathrm{d}z \times \exp\left[-\frac{\pi D}{2}(|a|^2+|b|^2-a^2-b^{*2}) + \mathrm{i}\pi(\mu-\nu-\alpha-\beta-\gamma)\right.$$

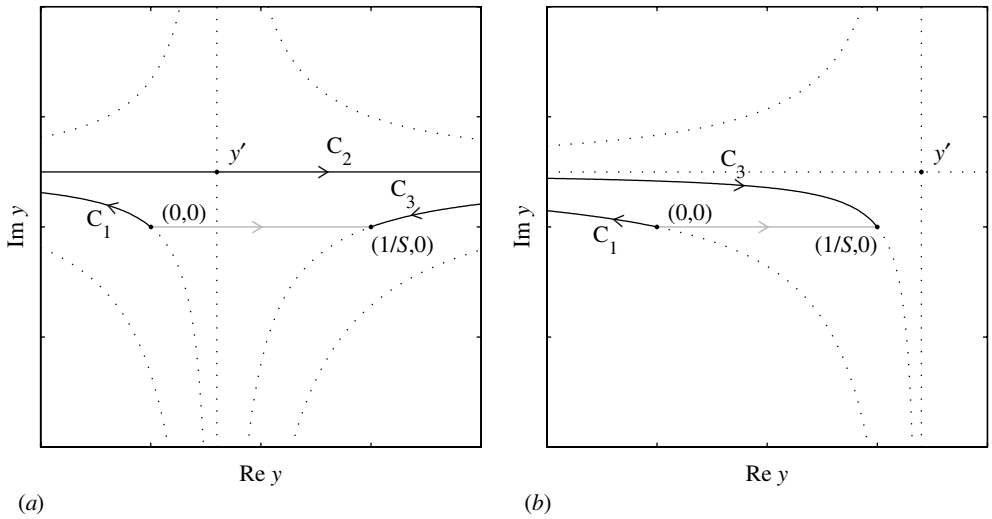

Figure 3. Steepest descent paths for $f(y)$. The original integration path along the real line (grey) is deformed to one where Im $f(y) =$ constant (black).

$$-\pi D(y + x_1/2 + m/S - a + \mu)^2 - \pi D(z + 2m/S - b^* + \nu)^2$$
$$+ \mathrm{i}\pi SD(xz + x_1 z/S - 2xy) + 2\mathrm{i}\pi D(x\alpha + y\beta + z\gamma)\Big]. \tag{23}$$

We are now ready to make a semi-classical approximation to our matrix element. More precisely, we will make a saddle-point approximation to the triple integral above. Only near a saddle-point will contributions from such an integral cancel the pre-factor $D^{3/2}$ and lead to an $O(1)$ contribution for the matrix element. The saddle-point approximation can be written immediately using well-known formulae found in any standard text [40]. However, the limits in the above integrals are finite; therefore the saddle point will not make a contribution in all cases. We need to consider this possibility carefully if we are to recover the classical baker's map. Hence, we will treat each one-dimensional integral separately and use the method of steepest descent.

Consider first the y integration (with x a parameter) by defining

$$I_1 \equiv \int_0^{1/S} \mathrm{d}y \exp[-\pi D f(y)] \tag{24}$$

where

$$f(y) \equiv (y - A)^2 + 2\mathrm{i}(Sx - \beta)y \tag{25}$$

$$A \equiv a - x_1/2 - m/S - \mu. \tag{26}$$

An asymptotic calculation of this integral is enabled by deforming the integration path, currently along the real line, to one in the complex plane where Im $f(y) =$ constant. Two important cases are drawn in figure 3. The first (a) occurs when the saddle point (defined through $f'(y') = 0$)

$$y' = A - \mathrm{i}Sx + \mathrm{i}\beta \tag{27}$$

satisfies $0 <$ Re $y' < 1/S$. In this case, the steepest descent path is one which first travels along the hyperbola C_1 from 0 to $-\infty +$ i Im y', then along the hyperbolic asymptote C_2 to

$\infty + \mathrm{i}\,\mathrm{Im}\,y'$, and finally back to $1/S$ via another hyperbola C_3. Hence an asymptotic expansion for the integral I_1 will be the sum of three parts, each associated with a different contour C_1, C_2 or C_3 in the complex plane. Note that along the contours C_1 and C_3, the kernel attains its maximum at the end points 0 and $1/S$, respectively. Consequently, the leading term in an asymptotic expansion takes the form

$$\frac{-1}{\pi D f'(c)} \exp[-\pi D f(c)][1 + O(1/D)] \tag{28}$$

with $c = 0$ or $1/S$. However, the pre-factor of $1/D$ in the above inhibits such terms from playing a role in the leading-order approximation of our matrix element. As remarked before, we need pre-factors of $D^{-1/2}$ in each approximation of the three integrals in (23) in order to obtain an $O(1)$ overall contribution for the matrix element. Hence, we will simply discard the integration along contours C_1 and C_3, and make the approximation

$$I_1 \approx \int_{-\infty+\mathrm{i}\,\mathrm{Im}\,y'}^{\infty+\mathrm{i}\,\mathrm{Im}\,y'} \mathrm{d}y \exp[-\pi D f(y)] \qquad \text{if} \quad 0 < \mathrm{Re}\,y' < 1/S \tag{29}$$

$$= D^{-1/2} \exp[-\pi D f(y')]. \tag{30}$$

When $\mathrm{Re}\,y' < 0$ or $\mathrm{Re}\,y' > 1/S$ (figure 3(*b*)) the path of steepest descent no longer passes through the saddle point, and consequently, there will be no leading-order contributions to the matrix element, i.e. we may set $I_1 = 0$. The third and final case occurs when $\mathrm{Re}\,y' = 0$ or $1/S$. One may investigate these possibilities by taking exactly one half of (30) as the approximation for I_1. However, for simplicity, we will not deal with this case, except make the odd casual remark when needed. In summary, we take (30) as our approximation for I_1 when $0 < \mathrm{Re}\,y' < 1/S$, and otherwise zero.

Similarly, for the z integration one has

$$I_2 \equiv \int_0^{2/S} \mathrm{d}z \exp[-\pi D g(z)] \tag{31}$$

$$\approx D^{-1/2} \exp[-\pi D g(z')] \qquad \text{if} \quad 0 < \mathrm{Re}\,z' < 2/S \tag{32}$$

with

$$g(z) \equiv (z - B)^2 - 2\mathrm{i}(Sx/2 + x_1/2 + \gamma)z \tag{33}$$

$$B \equiv b^* - 2m/S - v \tag{34}$$

and the saddle point is

$$z' = B + \mathrm{i}Sx/2 + \mathrm{i}x_1/2 + \mathrm{i}\gamma. \tag{35}$$

Now, letting x vary again and setting

$$h(x) \equiv f(y') + g(z') - 2\mathrm{i}\alpha x \tag{36}$$

$$= \tfrac{5}{4}S^2x^2 + S(2\mathrm{i}A - \mathrm{i}B + x_1/2 - 2\beta + \gamma - 2\mathrm{i}\alpha/S)x$$
$$- 2\mathrm{i}A\beta - \mathrm{i}B(x_1 + 2\gamma) + \beta^2 + (x_1/2 + \gamma)^2 \tag{37}$$

we have the final integral

$$I_3 \equiv \int_0^{1/S} \mathrm{d}x \exp[-\pi D h(x)] \tag{38}$$

$$\approx \sqrt{\frac{4}{5S^2D}} \exp[-\pi D h(x')] \qquad \text{if} \quad 0 < \mathrm{Re}\,x' < 1/S \tag{39}$$

with the saddle point at

$$x' = -\frac{2}{5S}(2\mathrm{i}A - \mathrm{i}B + x_1/2 - 2\beta + \gamma - 2\mathrm{i}\alpha/S). \tag{40}$$

Now, inserting our saddle-point approximations back into (23) and setting $a \equiv a_1 + \mathrm{i}a_2$ and $b \equiv b_1 + \mathrm{i}b_2$, with a little algebra we obtain

$$\begin{aligned}\langle b|\hat{B}_{0,s}|a\rangle \approx \sqrt{\frac{4}{5}} \sum_{\substack{\mu,\nu,\alpha \\ \beta,\gamma=-\infty}}^{\infty} \sum_{x_1=0}^{1} \sum_{m=0}^{S/2-1} \exp\Bigg[&-\frac{\pi D}{5}\{(2a_1 - b_1 - x_1 - 2\mu + \nu - 2\alpha/S)^2 \\ &+ (a_2 - 2b_2 + x_1 + \beta + 2\gamma)^2\} + \mathrm{i}\pi(\mu - \nu - \alpha - \beta - \gamma) + \mathrm{i}\pi D(a_1 a_2 - b_1 b_2) \\ &- \frac{2\mathrm{i}\pi D}{5}\{(2a_1 - b_1 - x_1 - 2\mu + \nu - 2\alpha/S)(2a_2 + b_2) \\ &- (a_1 + 2b_1 - x_1/2 - \mu - 2\nu)(x_1 + \beta + 2\gamma) + \alpha(x_1 - 4\beta + 2\gamma)/S\}\Bigg]\end{aligned} \tag{41}$$

provided that all three of the inequalities

$$0 < \mathrm{Re}\, x' = \frac{2}{5S}(2a_2 + b_2 - x_1/2 + 2\beta - \gamma) < \frac{1}{S} \tag{42}$$

$$0 < \mathrm{Re}\, y' = \frac{1}{5}(a_1 + 2b_1 - x_1/2 - \mu - 2\nu) + \frac{1}{5S}(4\alpha - 5m) < \frac{1}{S} \tag{43}$$

$$0 < \frac{1}{2}\mathrm{Re}\, z' = \frac{1}{5}(a_1 + 2b_1 - x_1/2 - \mu - 2\nu) - \frac{1}{5S}(\alpha + 5m) < \frac{1}{S} \tag{44}$$

are satisfied. Otherwise the summand is taken to be zero.

Note that although m no longer appears in the exponent, we cannot trivially evaluate the sum since not all values of m will satisfy (43) and (44). Consider the cases when approximation (41) becomes $O(1)$; that is,

$$2a_1 - b_1 - x_1 - 2\mu + \nu - 2\alpha/S = 0 \tag{45}$$

$$a_2 - 2b_2 + x_1 + \beta + 2\gamma = 0. \tag{46}$$

Substituting (46) into (42) we obtain

$$0 < a_2 + \beta < 1 \quad \text{or} \quad 0 < b_2 - x_1/2 - \gamma < \tfrac{1}{2} \tag{47}$$

and thus, the integers β and γ give our periodicity in the momentum direction. Hence if we assume $0 < a_2, b_2 < 1$ then we may set $\beta = \gamma = 0$ in (41), noting that we are discarding exponentially small Gaussian tails. Also note from (47) that we must have $x_1 = \lfloor 2b_2 \rfloor$.

Now, negating (44) and adding it to (43) we immediately arrive at the inequality $-1 < \alpha < 1$. Hence we must set $\alpha = 0$. This implies

$$\frac{2m}{S} < \frac{2}{5}(a_1 + 2b_1 - x_1/2 - \mu - 2\nu) < \frac{2(m+1)}{S} \tag{48}$$

from (43), (44), or equivalently

$$0 < \tfrac{2}{5}(a_1 + 2b_1 - x_1/2 - \mu - 2\nu) < 1 \tag{49}$$

if we now drop the summation over m in (41). Hence, following a similar procedure to the above, one can substitute (45) into the new inequality (49) and deduce that under the assumption $0 < a_1, b_1 < 1$, the summand of (41) becomes $O(1)$ only when $\mu = \nu = 0$. Furthermore, we will have $x_1 = \lfloor 2a_1 \rfloor$.

The surviving term of the summation is our semi-classical approximation for the propagator,

$$\langle b|\hat{B}_{0,s}|a\rangle = \sqrt{\frac{4}{5}}\exp\left[-\frac{\pi D}{5}\{(2a_1 - b_1 - \lfloor 2a_1\rfloor)^2 + (a_2 - 2b_2 + \lfloor 2a_1\rfloor)^2 + \mathrm{i}(3a_1a_2 + 3b_1b_2 + 4a_1b_2 - 4a_2b_1) - 2\mathrm{i}\lfloor 2a_1\rfloor(a_1 + 2b_1 + 2a_2 + b_2 - \lfloor 2a_1\rfloor/2)\}\right] + o(1) \tag{50}$$

where we have chosen $x_1 = \lfloor 2a_1\rfloor$ (and implicitly assumed $a_1 \neq \frac{1}{2}$ and $b_2 \neq \frac{1}{2}$ by ignoring cases of equality in (42)–(44)). All other terms in (41), being exponentially small, are discarded.

Note that the above approximation is $O(1)$ only when b is the iterate of a under the classical baker's map (3). Furthermore, a little algebra reveals that our semi-classical propagator may be rewritten in the Van Vleck form

$$\langle b|\hat{B}_{0,s}|a\rangle = \sqrt{\frac{\partial^2 W}{\partial a\,\partial b^*}}\exp[\pi D W(b^*, a)]\exp[-\pi D(|a|^2 + |b|^2)/2] + o(1) \tag{51}$$

where $W(b^*, a)$ is the classical generating function (4). Hence we have shown that the class of quantum baker's map with $\theta = 0$ will approach the classical baker's map in the limit $D \to \infty$.

3.2. *Case* $0 < \theta < 1$

We will now consider the case $0 < \theta < 1$. Using (16) and (17) with $n = \theta N + s$, our matrix element is

$$\begin{aligned}\langle b|\hat{B}_{\theta,s}|a\rangle = \frac{S}{\sqrt{D}D^{\phi}}\sum_{\mu,\nu=-\infty}^{\infty}\sum_{x_1=0}^{1}\sum_{j,k=0}^{D^{\phi}/S-1}\sum_{l=0}^{2D^{\phi}/S-1}\sum_{m=0}^{SD^{\theta}/2-1}\exp\Bigg[&-\frac{\pi D}{2}(|a|^2 + |b|^2 - a^2 - b^{*2}) \\ &+ \mathrm{i}\pi(\mu - \nu) - \pi D\big(\big(q_k^{\phi} - 1/2S\big)/D^{\theta} + x_1/2 + q_m^{\theta}/S - a + \mu\big)^2 \\ &- \pi D\big(\big(q_l^{\phi} - 1/S\big)/D^{\theta} + 2q_m^{\theta}/S - b^* + \nu\big)^2 \\ &+ \mathrm{i}\pi SD^{\phi}\big(q_j^{\phi}q_l^{\phi} + x_1q_l^{\phi}/S - 2q_j^{\phi}q_k^{\phi}\big)\Bigg]\end{aligned} \tag{52}$$

where again $S \equiv 2^s$. Introducing the new summing variables $q_m^{\theta} \equiv q_m D/D^{\theta}$, $q_j^{\phi} \equiv q_j D/D^{\phi}$ etc enables us to convert the four finite sums over j, k, l and m to integrals over x, y, z and t, respectively, using formulae similar to (22). The result is

$$\begin{aligned}\langle b|\hat{B}_{\theta,s}|a\rangle = S\sqrt{D}D^{\phi}\sum_{\substack{\mu,\nu,\alpha,\beta\\ \gamma,\kappa=-\infty}}^{\infty}\sum_{x_1=0}^{1}\int_0^{1/S}\mathrm{d}x\int_0^{1/S}\mathrm{d}y\int_0^{2/S}\mathrm{d}z\int_0^{S/2}\mathrm{d}t\exp\Bigg[&-\frac{\pi D}{2}(|a|^2 + |b|^2 \\ &- a^2 - b^{*2}) + \mathrm{i}\pi(\mu - \nu - \alpha - \beta - \gamma - \kappa) - \pi D((y - 1/2S)/D^{\theta} \\ &+ x_1/2 + t/S - a + \mu)^2 - \pi D((z - 1/S)/D^{\theta} + 2t/S - b^* + \nu)^2 \\ &+ \mathrm{i}\pi SD^{\phi}(xz + x_1z/S - 2xy) + 2\mathrm{i}\pi D^{\phi}(x\alpha + y\beta + z\gamma) + 2\mathrm{i}\pi D^{\theta}t\kappa\Bigg]\end{aligned} \tag{53}$$

$$= \frac{\sqrt{D}D^{\phi}}{S} \sum_{\substack{\mu,\nu,\alpha,\beta \\ \gamma,\kappa=-\infty}}^{\infty} \sum_{x_1=0}^{1} \int_0^1 \mathrm{d}x \int_0^1 \mathrm{d}y \int_0^2 \mathrm{d}z \int_0^{1/2} \mathrm{d}t \exp\Bigg[-\frac{\pi D}{2}(|a|^2 + |b|^2$$
$$- a^2 - b^{*2}) + \mathrm{i}\pi(\mu - \nu - \alpha - \beta - \gamma - \kappa) - \pi D(t + x_1/2 - a + \mu)^2$$
$$- \pi D(2t - b^* + \nu)^2 - 2\pi D^{\phi}\left(y - \tfrac{1}{2}\right)(t + x_1/2 - a + \mu)/S - 2\pi D^{\phi}(z-1)$$
$$\times (2t - b^* + \nu)/S + \mathrm{i}\pi D^{\phi}(xz + x_1 z - 2xy)/S + 2\mathrm{i}\pi D^{\phi}(x\alpha + y\beta + z\gamma)/S$$
$$- \pi D^{\phi-\theta}\left(y - \tfrac{1}{2}\right)^2/S^2 - \pi D^{\phi-\theta}(z-1)^2/S^2 + 2\mathrm{i}\pi S D^{\theta} t\kappa \Bigg] \tag{54}$$

where we have rescaled the integration variables ($x \to x/S$, $y \to y/S$, $z \to z/S$ and $t \to tS$), then collected terms in the exponent with the same power of D. The terms with highest power are those containing t, and hence, we will consider the integration over this variable first. Define the integral

$$I_4 \equiv \int_0^{1/2} \mathrm{d}t \exp[-\pi D(t - A)^2 - \pi D(2t - B)^2 - 2\pi D^{\phi} tC + 2\mathrm{i}\pi S D^{\theta} t\kappa] \tag{55}$$

where the constants are

$$A \equiv a - x_1/2 - \mu \tag{56}$$
$$B \equiv b^* - \nu \tag{57}$$
$$C \equiv \left(y - \tfrac{1}{2}\right)\Big/ S + 2(z-1)/S. \tag{58}$$

We now wish to derive the contribution from I_4 which gives the leading-order approximation to our matrix element. This is done by taking a path of steepest descent for the function $f(t) \equiv (t - A)^2 + (2t - B)^2$. Note that when $\phi = 1$ the third term of the exponent in (55) also becomes dominant and must be incorporated into $f(t)$. Hence the need to consider this case separately in the previous section.

As before, we may discard all parts of our integration contour, except the segment $(-\infty + \mathrm{i}\,\mathrm{Im}\,t', \infty + \mathrm{i}\,\mathrm{Im}\,t')$ which passes through the saddle point

$$t' = \frac{A + 2B}{5}. \tag{59}$$

It is only this contribution which will cancel the pre-factor $\sqrt{D}D^{\phi}$ in (54) to give an $O(1)$ overall contribution to the matrix element. Hence we make the approximation

$$I_4 \approx \int_{-\infty+\mathrm{i}\,\mathrm{Im}\,t'}^{\infty+\mathrm{i}\,\mathrm{Im}\,t'} \mathrm{d}t \exp[-\pi D(t - A)^2 - \pi D(2t - B)^2 - 2\pi D^{\phi} tC + 2\mathrm{i}\pi S D^{\theta} t\kappa] \tag{60}$$

$$= \frac{1}{\sqrt{5D}} \exp\Bigg[-\frac{\pi D}{5}(2A - B)^2 - \frac{2\pi D^{\phi}}{5}(A + 2B)C$$
$$+ \frac{2\mathrm{i}\pi D^{\theta}}{5}(A + 2B)S\kappa + \frac{\pi D^{\phi-\theta}}{5}C^2 - \frac{\pi D^{\theta-\phi}}{5}S^2\kappa^2 - \frac{2\mathrm{i}\pi}{5}CS\kappa \Bigg] \tag{61}$$

if $0 < \mathrm{Re}\,t' < \frac{1}{2}$, and otherwise zero.

Substituting this approximation back into (54) and simplifying, we obtain

$$\langle b|\hat{B}_{\theta,s}|a\rangle \approx \frac{D^{\phi}}{\sqrt{5}S} \sum_{\substack{\mu,\nu,\alpha,\beta \\ \gamma,\kappa=-\infty}}^{\infty} \sum_{x_1=0}^{1} \int_0^1 \mathrm{d}x \int_0^1 \mathrm{d}y \int_0^2 \mathrm{d}z \exp\Bigg[-\frac{\pi D}{2}(|a|^2 + |b|^2 - a^2 - b^{*2})$$
$$+ \mathrm{i}\pi(\mu - \nu - \alpha - \beta - \gamma) - \frac{\pi D}{5}(2A - B)^2 + \frac{2\pi D^{\phi}}{5S}(2A - B)(2y - z)$$

$$+\frac{\mathrm{i}\pi D^{\phi}}{S}(xz+x_1z-2xy)+\frac{2\mathrm{i}\pi D^{\phi}}{S}(x\alpha+y\beta+z\gamma)-\frac{\pi D^{\phi-\theta}}{5S^2}(2y-z)^2$$
$$-\frac{2\mathrm{i}\pi}{5}(y+2z)\kappa+\frac{2\mathrm{i}\pi D^{\theta}}{5}(A+2B)S\kappa-\frac{\pi D^{\theta-\phi}}{5}S^2\kappa^2\Bigg]. \tag{62}$$

The dominant terms in the exponent which contain the integration variables are now those with D^{ϕ} as a pre-factor. These terms do not define a saddle point, but instead, a line. Hence, it is advantageous to first decouple x, y and z in these terms using the following transformation,

$$\begin{bmatrix} u \\ v \\ w \end{bmatrix} = \begin{bmatrix} 1 & -2 & 1 \\ 1 & 2 & -1 \\ 0 & 1 & 2 \end{bmatrix} \begin{bmatrix} x \\ y \\ z \end{bmatrix} \tag{63}$$

where the integration region $(x, y, z) \in [0, 1] \times [0, 1] \times [0, 2]$ is transformed to some parallelepiped Ω.

After making this transformation, equation (62) may be rewritten in the form

$$\langle b|\hat{B}_{\theta,s}|a\rangle \approx \frac{D^{\phi}}{10\sqrt{5}S}\sum_{\substack{\mu,\nu,\alpha,\beta \\ \gamma,\kappa=-\infty}}^{\infty}\sum_{x_1=0}^{1}\iiint_{\Omega}\mathrm{d}u\,\mathrm{d}v\,\mathrm{d}w$$
$$\times\exp\left[-\frac{\pi D^{\phi}}{S}g(u)-\frac{\pi D^{\phi}}{S}h(v)-\frac{\pi D^{\phi-\theta}}{20S^2}(u-v)^2\right]F(w) \tag{64}$$

where

$$g(u)\equiv-\frac{\mathrm{i}}{4}u^2-(E+\mathrm{i}\alpha)u \tag{65}$$

$$h(v)\equiv\frac{\mathrm{i}}{4}v^2+(E-\mathrm{i}\alpha)v \tag{66}$$

$$E\equiv-\frac{1}{5}(2A-B)+\frac{\mathrm{i}}{5}(x_1/2-2\beta+\gamma)\equiv E_1+\mathrm{i}E_2 \tag{67}$$

and

$$F(w)\equiv\exp\Bigg[-\frac{\pi D}{2}(|a|^2+|b|^2-a^2-b^{*2})+\mathrm{i}\pi(\mu-\nu-\alpha-\beta-\gamma)-\frac{\pi D}{5}(2A-B)^2$$
$$+\frac{2\mathrm{i}\pi D^{\theta}}{5}(A+2B)S\kappa-\frac{\pi D^{\theta-\phi}}{5}S^2\kappa^2+\frac{2\mathrm{i}\pi}{5S}(D^{\phi}(x_1+\beta+2\gamma)-S\kappa)w\Bigg]. \tag{68}$$

We have now arrived at a form where we can consider steepest descent paths for the integration variables u and v. Starting our program with the function $g(u)$ and writing u in terms of its real and imaginary parts $u = u_1+\mathrm{i}u_2$, one finds that the two hyperbolic asymptotes

$$u_1-u_1'=u_2-u_2' \tag{69}$$
$$u_1-u_1'=-u_2+u_2' \tag{70}$$

are the steepest descent paths which pass through the saddle point

$$u'=u_1'+\mathrm{i}u_2'=2(\mathrm{i}E-\alpha). \tag{71}$$

However, only the first (69) can be used as an integration contour, since $\exp[-\pi D^{\phi}\,\mathrm{Re}\,g(u)/S]\to\infty$ on the other. Cases for when this asymptote (denoted by C_2) is required to form part of the integration contour, and when it is not, are plotted in

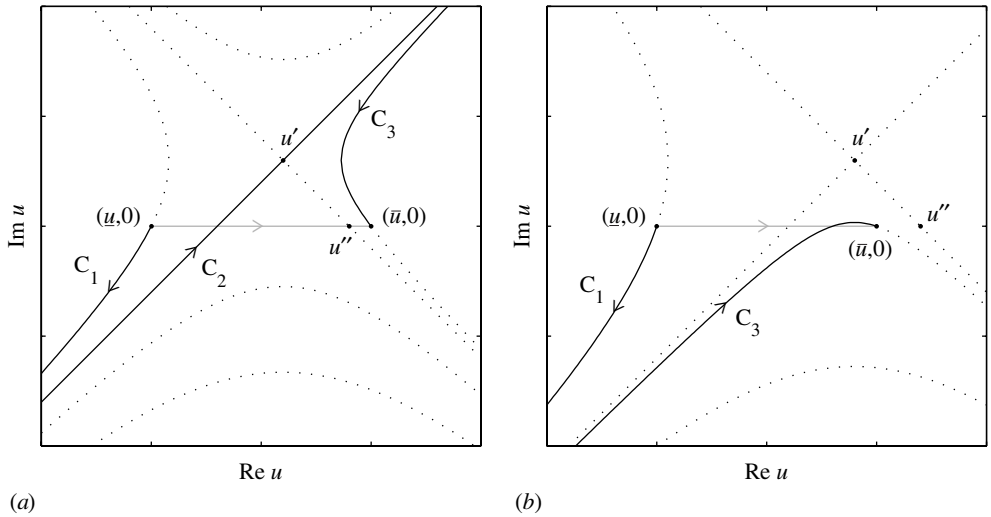

Figure 4. Steepest descent paths for $g(u)$.

figures 4(a) and (b), respectively. Here the integration limits are denoted by the real numbers $\underline{u}$ and $\overline{u}$, and need not be known explicitly for the moment. Note that C_2 is included in the contour only when the intercept of the second asymptote (70) with the real line, denoted by u'', is between these limits; that is

$$\underline{u} < u'' = u_1' + u_2' = 2(E_1 - E_2 - \alpha) < \overline{u}. \tag{72}$$

The importance of this inequality is not clear yet. We shall return to it after transforming back to our x, y and z variables.

The analysis of $h(v)$ is very similar. In this case, one finds that our steepest descent path will travel along the asymptote

$$v_1 - v_1' = -v_2 + v_2' \tag{73}$$

and hence, through the saddle point

$$v' = v_1' + \mathrm{i}v_2' = 2(\mathrm{i}E + \alpha) \tag{74}$$

only when

$$\underline{v} < v'' = v_1' - v_2' = 2(\alpha - E_1 - E_2) < \overline{v}. \tag{75}$$

But what are our integration limits $\underline{u}$, $\overline{u}$, $\underline{v}$ and $\overline{v}$? Unfortunately, given the nature of the variable change, their values differ as one integrates over the volume element Ω. Therefore, it is convenient to convert back to our original variables x, y and z which have independent limits. We know that whenever the point (u'', v'', w) belongs to our integration region Ω, the two contours (69) and (73) will be included in our integration path of steepest descent. Therefore, by inverting our transformation (63), we obtain

$$\begin{array}{lcl} u'' = 2(E_1 - E_2 - \alpha) & & x'' = -2E_2 \\ v'' = 2(\alpha - E_1 - E_2) & \Rightarrow & y'' = \frac{4}{5}(\alpha - E_1) + \frac{1}{5}w \\ w = w & & z'' = -\frac{2}{5}(\alpha - E_1) + \frac{2}{5}w \end{array} \tag{76}$$

and hence, the condition $(u'', v'', w) \in \Omega$ is equivalent to

$$0 < x'' < 1 \tag{77}$$

$$0 < y'' < 1 \tag{78}$$

$$0 < z'' < 2. \tag{79}$$

Inequalities (78) and (79) may be rewritten as

$$\alpha - E_1 < w < 5 + \alpha - E_1 \tag{80}$$

$$-4(\alpha - E_1) < w < 5 - 4(\alpha - E_1) \tag{81}$$

which asserts that

$$\underline{w} < w < \overline{w} \tag{82}$$

where $\underline{w} \equiv \max\{\alpha - E_1, -4(\alpha - E_1)\}$ and $\overline{w} \equiv 5 + \min\{\alpha - E_1, -4(\alpha - E_1)\}$. The requirement that $\underline{w} < \overline{w}$ implies

$$-1 < \alpha - E_1 < 1. \tag{83}$$

Having learned all we can from the method of steepest descent about the restrictions placed upon our integration parameters, we may proceed with the saddle-point approximation of (64). This is done by discarding all contours which do not make a contribution to the leading-order approximation of our matrix element (e.g. for u, we discard C_1 and C_3 in figure 4). Hence

$$\langle b|\hat{B}_{\theta,s}|a\rangle \approx \frac{D^{\phi}}{10\sqrt{5}S} \sum_{\substack{\mu,\nu,\alpha,\beta \\ \gamma,\kappa=-\infty}}^{\infty} \sum_{x_1=0}^{1} \int_{u'-\infty e^{i\pi/4}}^{u'+\infty e^{i\pi/4}} du \int_{v'-\infty e^{-i\pi/4}}^{v'+\infty e^{-i\pi/4}} dv \int_{\underline{w}}^{\overline{w}} dw$$
$$\times \exp\left[-\frac{\pi D^{\phi}}{S} g(u) - \frac{\pi D^{\phi}}{S} h(v) - \frac{\pi D^{\phi-\theta}}{20S^2}(u-v)^2\right] F(w) \tag{84}$$

$$= \frac{1}{5}\sqrt{\frac{4}{5}} \sum_{\substack{\mu,\nu,\alpha,\beta \\ \gamma,\kappa=-\infty}}^{\infty} \sum_{x_1=0}^{1} \int_{\underline{w}}^{\overline{w}} dw \exp\left[-\frac{\pi D}{2}(|a|^2 + |b|^2 - a^2 - b^{*2})\right.$$
$$+ i\pi(\mu - \nu - \alpha - \beta - \gamma) - \frac{\pi D}{5}(2A - B)^2 - \frac{4\pi D^{\phi}}{S} E\alpha - \frac{4\pi D^{\phi-\theta}}{5S^2}\alpha^2$$
$$\left. + \frac{2i\pi D^{\theta}}{5}(A + 2B)S\kappa - \frac{\pi D^{\theta-\phi}}{5} S^2\kappa^2 + \frac{2i\pi}{5S}(D^{\phi}(x_1 + \beta + 2\gamma) - S\kappa)w\right]. \tag{85}$$

Note that we have actually made a saddle-point approximation about a line parametrized by w, over which we still need to integrate. Currently, there are no restrictions placed upon κ. However, the integral over w will be $O(D^{-\phi})$ unless $\kappa = D^{\phi}(x_1 + \beta + 2\gamma)/S$. We may set κ to this value by noting that we are only shifting the saddle point t' by the imaginary amount $i\pi(x_1 + \beta + 2\gamma)$ (see equation (55)), and thus, our approximation of I_4 (61) is unchanged.

Hence, putting $\kappa = D^{\phi}(x_1 + \beta + 2\gamma)/S$ and integrating over w, we arrive at

$$\langle b|\hat{B}_{\theta,s}|a\rangle \approx \frac{1}{5}\sqrt{\frac{4}{5}} \sum_{\substack{\mu,\nu,\alpha,\beta \\ \gamma=-\infty}}^{\infty} \sum_{x_1=0}^{1} (\overline{w} - \underline{w}) \exp\left[-\frac{\pi D}{5}\{(2a_1 - b_1 - x_1 - 2\mu + \nu)^2\right.$$
$$\left. + (a_2 - 2b_2 + x_1 + \beta + 2\gamma)^2\} + i\pi(\mu - \nu - \alpha - \beta - \gamma) + i\pi D(a_1 a_2 - b_1 b_2)\right.$$

$$-\frac{2\mathrm{i}\pi D}{5}\{(2a_1-b_1-x_1-2\mu+\nu)(2a_2+b_2)-(a_1+2b_1-x_1/2 \\ -\mu-2\nu)(x_1+\beta+2\gamma)\}-\frac{4\pi D^{\phi}}{S}E\alpha-\frac{4\pi D^{\phi-\theta}}{5S^2}\alpha^2\Bigg] \tag{86}$$

provided that all three of the inequalities

$$0<x''=\tfrac{2}{5}(2a_2+b_2-x_1/2+2\beta-\gamma)<1 \tag{87}$$

$$0<2\,\mathrm{Re}\,t'=\tfrac{2}{5}(a_1+2b_1-x_1/2-\mu-2\nu)<1 \tag{88}$$

$$-1<\alpha+\tfrac{1}{5}(2a_1-b_1-x_1-2\mu+\nu)<1 \tag{89}$$

are satisfied. Otherwise the summand is taken to be zero.

Again, in a similar fashion to the previous section, we note that if the above approximation is to become $O(1)$, we must set $2a_1-b_1-x_1-2\mu+\nu=0$ and $a_2-2b_2+x_1+\beta+2\gamma=0$. Consequently, under the assumption $0<a_1,a_2,b_1,b_2<1$, the above three inequalities will now require us to set $\mu=\nu=\alpha=\beta=\gamma=0$ and $x_1=\lfloor 2a_1\rfloor$. Furthermore, we assume $a_1\neq\frac{1}{2}$ and $b_2\neq\frac{1}{2}$ by ignoring cases of equality in (87)–(89).

Thus, by discarding all exponentially small terms, we arrive at the semi-classical propagator

$$\langle b|\hat{B}_{\theta,s}|a\rangle=\sqrt{\frac{4}{5}}\left(1-\frac{1}{5}|2a_1-b_1-\lfloor 2a_1\rfloor|\right)\exp\Bigg[-\frac{\pi D}{5}\{(2a_1-b_1-\lfloor 2a_1\rfloor)^2 \\ +(a_2-2b_2+\lfloor 2a_1\rfloor)^2+\mathrm{i}(3a_1a_2+3b_1b_2+4a_1b_2-4a_2b_1) \\ -2\mathrm{i}\lfloor 2a_1\rfloor(a_1+2b_1+2a_2+b_2-\lfloor 2a_1\rfloor/2)\}\Bigg]+o(1) \tag{90}$$

$$=\sqrt{\frac{4}{5}}\exp\Bigg[-\frac{\pi D}{5}\{(2a_1-b_1-\lfloor 2a_1\rfloor)^2+(a_2-2b_2+\lfloor 2a_1\rfloor)^2+\mathrm{i}(3a_1a_2+3b_1b_2 \\ +4a_1b_2-4a_2b_1)-2\mathrm{i}\lfloor 2a_1\rfloor(a_1+2b_1+2a_2+b_2-\lfloor 2a_1\rfloor/2)\}\Bigg]+o(1). \tag{91}$$

Both forms, (90) and (91), are equally valid since their difference is exponentially small (although the first, (90), may prove to be more accurate). Comparing (91) to (50), we see that for $0<\theta<1$, the semi-classical propagator also takes the Van Vleck form (51). Furthermore, the classical baker's map will be recovered in the limit $D\to\infty$.

3.3. Case $\theta=1$

After the rousing success of the previous calculations, it is tempting to conclude that the classical baker's map will always be restored in the limit $D\to\infty$. Unfortunately, when $\theta=1$ ($\phi=0$), certain assumptions made previously will prove incorrect. In particular, in equation (62), we have assumed that D^{ϕ} terms will dominate; however this clearly cannot be the case now. In this section, we show that such differences cripple any hope that the classical baker's map will be recovered for all possible classical limits.

When $\theta=1$ the number of momentum bits $r\equiv -s\geqslant 0$ remains constant. Using (16) and (17), with $n=N-r$ and $R\equiv 2^r$, our matrix element is

$$\langle b|\hat{B}_{1,-r}|a\rangle=\frac{1}{\sqrt{D}R}\sum_{\mu,\nu=-\infty}^{\infty}\sum_{x_1=0}^{1}\sum_{j,k=0}^{R-1}\sum_{l=0}^{2R-1}\sum_{m=0}^{D/(2R)-1}\exp\Bigg[-\frac{\pi D}{2}(|a|^2+|b|^2-a^2-b^{*2}) \\ +\mathrm{i}\pi(\mu-\nu)-\pi D\left(Rq_m+x_1/2-a+\mu+\left(k+\tfrac{1}{2}-R/2\right)\Big/D\right)^2$$

$$- \pi D \left(2Rq_m - b^* + \nu + \left(l + \tfrac{1}{2} - R\right)/\, D\right)^2 + \frac{\mathrm{i}\pi}{R}\left\{\left(j + \tfrac{1}{2}\right)\left(l + \tfrac{1}{2}\right) + Rx_1\left(l + \tfrac{1}{2}\right) - 2\left(j + \tfrac{1}{2}\right)\left(k + \tfrac{1}{2}\right)\right\}\Bigg] \tag{92}$$

$$= \frac{\sqrt{D}}{R^2} \sum_{\mu,\nu,\kappa=-\infty}^{\infty} \sum_{x_1=0}^{1} \sum_{j,k=0}^{R-1} \sum_{l=0}^{2R-1} \int_0^{1/2} \mathrm{d}t \exp\Bigg[-\frac{\pi D}{2}(|a|^2 + |b|^2 - a^2 - b^{*2}) + \mathrm{i}\pi(\mu - \nu - \kappa) - \pi D(t + x_1/2 - a + \mu)^2 - \pi D(2t - b^* + \nu)^2 - \frac{\pi}{D}\left(k + \tfrac{1}{2} - R/2\right)^2 - \frac{\pi}{D}\left(l + \tfrac{1}{2} - R\right)^2 + \frac{2\mathrm{i}\pi D}{R} t\kappa - 2\pi(t + x_1/2 - a + \mu)\left(k + \tfrac{1}{2} - R/2\right) - 2\pi(2t - b^* + \nu)\left(l + \tfrac{1}{2} - R\right) + \frac{\mathrm{i}\pi}{R}\left\{\left(j + \tfrac{1}{2}\right)\left(l + \tfrac{1}{2}\right) + Rx_1\left(l + \tfrac{1}{2}\right) - 2\left(j + \tfrac{1}{2}\right)\left(k + \tfrac{1}{2}\right)\right\}\Bigg] \tag{93}$$

where we have converted the sum over m to an integral over t using the same technique as in the previous sections.

Now defining the integral

$$I_5 \equiv \int_0^{1/2} \mathrm{d}t \exp\left[-\pi D f(t) - 2\pi(t - A)\left(k + \tfrac{1}{2} - R/2\right) - 2\pi(2t - B)\left(l + \tfrac{1}{2} - R\right)\right] \tag{94}$$

where

$$f(t) \equiv (t - A)^2 + (2t - B)^2 - 2\mathrm{i}t\kappa/R \tag{95}$$

$$A \equiv a - x_1/2 - \mu \tag{96}$$

$$B \equiv b^* - \nu \tag{97}$$

one finds the saddle point

$$t' = \frac{A + 2B}{5} + \frac{\mathrm{i}\kappa}{5R} \tag{98}$$

and hence, the approximation

$$I_5 \approx \int_{-\infty + \mathrm{i}\,\mathrm{Im}\,t'}^{\infty + \mathrm{i}\,\mathrm{Im}\,t'} \mathrm{d}t \exp\left[-\pi D f(t) - 2\pi(t - A)\left(k + \tfrac{1}{2} - R/2\right) - 2\pi(2t - B)\left(l + \tfrac{1}{2} - R\right)\right] \tag{99}$$

$$= \frac{1}{\sqrt{5D}} \exp\Bigg[-\frac{\pi D}{5}(2A - B)^2 + \frac{2\mathrm{i}\pi D}{5R}(A + 2B)\kappa - \frac{\pi D}{5R^2}\kappa^2 + \mathrm{i}\pi\kappa + \frac{2\pi}{5}(2A - B)\left(2k - l + \tfrac{1}{2}\right) - \frac{2\mathrm{i}\pi}{5R}\left(k + 2l + \tfrac{3}{2}\right)\kappa + \frac{\pi}{5D}\left(k + 2l + \tfrac{3}{2} - 5R/2\right)^2\Bigg] \tag{100}$$

provided that $0 < \mathrm{Re}\, t' < \frac{1}{2}$, and otherwise zero.

Apart from the last term in the exponent, equation (100) is simply the well-known formula for a saddle-point approximation found in any standard text. We will now drop this $1/D$ term, along with all others in (93), to obtain the approximation

$$\langle b|\hat{B}_{1,-r}|a\rangle \approx \frac{1}{\sqrt{5}R^2} \sum_{\mu,\nu,\kappa=-\infty}^{\infty} \sum_{x_1=0}^{1} \sum_{j,k=0}^{R-1} \sum_{l=0}^{2R-1} \exp\Bigg[-\frac{\pi D}{5}\{(2a_1 - b_1 - x_1 - 2\mu + \nu)^2 + (a_2 - 2b_2 + \kappa/R)^2\} + \mathrm{i}\pi(\mu - \nu) + \mathrm{i}\pi D(a_1 a_2 - b_1 b_2) - \frac{2\mathrm{i}\pi D}{5}\{(2a_1 - b_1$$

$$
\begin{aligned}
&- x_1 - 2\mu + \nu)(2a_2 + b_2) - (a_1 + 2b_1 - x_1/2 - \mu - 2\nu)\kappa/R\} \\
&+ \frac{2\pi}{5}(2A - B)\left(2k - l + \tfrac{1}{2}\right) - \frac{2\mathrm{i}\pi}{5R}\left(k + 2l + \tfrac{3}{2}\right)\kappa \\
&+ \frac{\mathrm{i}\pi}{R}\left\{\left(j + \tfrac{1}{2}\right)\left(l + \tfrac{1}{2}\right) + Rx_1\left(l + \tfrac{1}{2}\right) - 2\left(j + \tfrac{1}{2}\right)\left(k + \tfrac{1}{2}\right)\right\}\Bigg] \qquad (101)
\end{aligned}
$$

if

$$
0 < 2\,\mathrm{Re}\,t' = \tfrac{2}{5}(a_1 + 2b_1 - x_1/2 - \mu - 2\nu) < 1 \qquad (102)
$$

and otherwise zero.

As in the previous cases, under the assumption $0 < a_1, b_1 < 1$, we may use (102) to set $\mu = \nu = 0$ and $x_1 = \lfloor 2a_1 \rfloor$. Thus, we arrive at the following semi-classical approximation for our propagator:

$$
\begin{aligned}
\langle b|\hat{B}_{1,-r}|a\rangle = \frac{1}{\sqrt{5}R^2}\sum_{\kappa=-\infty}^{\infty}\sum_{j,k=0}^{R-1}\sum_{l=0}^{2R-1}\exp\Bigg[&-\frac{\pi D}{5}\{(2a_1 - b_1 - \lfloor 2a_1\rfloor)^2 + (a_2 - 2b_2 + \kappa/R)^2 \\
&+ \mathrm{i}(3a_1a_2 + 3b_1b_2 + 4a_1b_2 - 4a_2b_1) - 2\mathrm{i}\kappa(a_1 + 2b_1 - \lfloor 2a_1\rfloor/2)/R - 2\mathrm{i}\lfloor 2a_1\rfloor \\
&\times (2a_2 + b_2)\} + \frac{2\pi}{5}(2a - b^* - \lfloor 2a_1\rfloor)\left(2k - l + \tfrac{1}{2}\right) - \frac{2\mathrm{i}\pi}{5R}\left(k + 2l + \tfrac{3}{2}\right)\kappa \\
&+ \frac{\mathrm{i}\pi}{R}\left\{\left(j + \tfrac{1}{2}\right)\left(l + \tfrac{1}{2}\right) + R\lfloor 2a_1\rfloor\left(l + \tfrac{1}{2}\right) - 2\left(j + \tfrac{1}{2}\right)\left(k + \tfrac{1}{2}\right)\right\}\Bigg] + o(1). \qquad (103)
\end{aligned}
$$

Note that the summation index κ remains unconstrained. Consequently, additional probabilistic 'humps' emerge at locations other than those specified by the classical bakers's map. In fact, in the region $0 < b_1, b_2 < 1$, there will be $2R$ humps at the positions $(b_1, b_2) = (2a_1 - \lfloor 2a_1\rfloor, (a_2 + \kappa/R)/2)$ where $-a_2R < \kappa < 2R - a_2R$.

Consider the simplest case $r = 0$. Our semi-classical propagator is then

$$
\begin{aligned}
\langle b|\hat{B}_{1,0}|a\rangle = \sqrt{\frac{4}{5}}\sum_{\kappa=0}^{1}\exp\Bigg[&-\frac{\pi D}{5}\{(2a_1 - b_1 - \lfloor 2a_1\rfloor)^2 \\
&+ (a_2 - 2b_2 + \kappa)^2 + \mathrm{i}(3a_1a_2 + 3b_1b_2 + 4a_1b_2 - 4a_2b_1) \\
&- 2\mathrm{i}\kappa(a_1 + 2b_1 - \lfloor 2a_1\rfloor/2) - 2\mathrm{i}\lfloor 2a_1\rfloor(2a_2 + b_2)\} + \mathrm{i}\pi(\lfloor 2a_1\rfloor - \kappa)\Bigg] \\
&\times \cos\left[\frac{\mathrm{i}\pi}{5}(2a - b^* - \lfloor 2a_1\rfloor) + \frac{\pi}{2}\left(\lfloor 2a_1\rfloor + \tfrac{1}{2}\right) - \frac{2\pi}{5}\kappa\right] + o(1) \qquad (104)
\end{aligned}
$$

defining two humps: one at a position specified by the classical baker's map, $(b_1, b_2) = (2a_1 - \lfloor 2a_1\rfloor, (a_2 + \lfloor 2a_1\rfloor)/2)$, with an asymptotic size

$$
|\langle b(a)|\hat{B}_{1,0}|a\rangle|^2 = \frac{4}{5}\cos^2\left[\frac{\pi}{2}\left(a_2 - \tfrac{1}{2}\right)\right] + o(1) \qquad (105)
$$

and another at $(b_1, b_2) = (2a_1 - \lfloor 2a_1\rfloor, (a_2 + 1 - \lfloor 2a_1\rfloor)/2)$ with the size

$$
|\langle b(a)|\hat{B}_{1,0}|a\rangle|^2 = \frac{4}{5}\sin^2\left[\frac{\pi}{2}\left(a_2 - \tfrac{1}{2}\right)\right] + o(1). \qquad (106)
$$

One interpretation of these equations could be that a *stochastic* mapping is implied in the classical limit: a point at (a_1, a_2) has the probability $\cos^2\left[\pi\left(a_2 - \frac{1}{2}\right)/2\right]$ of obeying the classical baker's map, and probability $\sin^2\left[\pi\left(a_2 - \frac{1}{2}\right)/2\right]$ of ending up at $(2a_1 - \lfloor 2a_1\rfloor, (a_2 + 1 - \lfloor 2a_1\rfloor)/2)$. Note that there is now a smooth transition of probabilities as one crosses the lines $a_2 = 0, 1$.

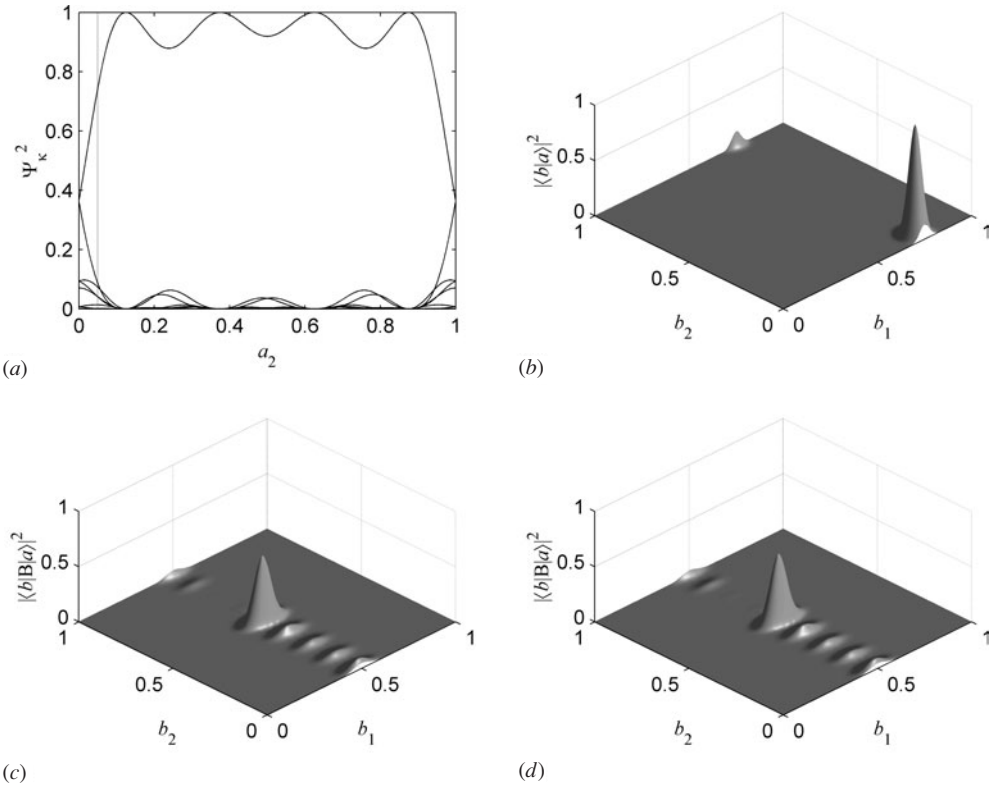

Figure 5. (*a*) The probabilities Ψ_κ^2 when $r = 2$. The Husimi functions of (*b*) the initial state $|a\rangle$ ($a = \frac{3}{4} + \mathrm{i}/20$), (*c*) its mapping $\hat{B}|a\rangle$, and (*d*) our semi-classical approximation (103), when $r = 2$ and $N = 8$. The humps have the height $\frac{4}{5}\Psi_\kappa^2$ with $a_2 = \frac{1}{20}$ (grey line in (*a*)).

Consider the size of our probabilistic humps in the general case. If we set $(b_1, b_2) = (2a_1 - \lfloor 2a_1 \rfloor, (a_2 + \kappa/R)/2)$, with κ fixed, then

$$\langle b(a)|\hat{B}_{1,-r}|a\rangle = \sqrt{\frac{4}{5}} \exp\left[\frac{\mathrm{i}\pi D}{2R}(2a_1\kappa + R\lfloor 2a_1 \rfloor a_2 - \lfloor 2a_1 \rfloor \kappa)\right] \Psi_\kappa(a) + o(1) \tag{107}$$

where

$$\Psi_\kappa(a) = \frac{1}{2R^2} \sum_{j=0}^{R-1} \frac{\cos^2[\pi R a_2]}{\sin\left[\pi\left(a_2 - \left(j + \frac{1}{2}\right)/R\right)\right] \sin\left[\frac{\pi}{2}(a_2 - \lfloor 2a_1 \rfloor + \kappa/R - \left(j + \frac{1}{2}\right)/R)\right]}. \tag{108}$$

The probability associated with each hump is given by Ψ_κ^2, with $\sum_{\kappa=0}^{2R-1} \Psi_\kappa^2 = 1$, and is plotted for $r = 2$ in figure 5(*a*). The curve with the largest probabilities is that associated with the 'correct' hump prescribed by the classical baker's map ($\kappa' = \lfloor 2a_1 \rfloor R$). It takes maximum values of unity whenever $a_2 = \left(m + \frac{1}{2}\right)/R$ ($0 < m < R - 1$), and as the number of momentum bits ($r = \log_2 R$) becomes large, $\Psi_{\kappa'}^2 \to 1$ for all $0 < a_2 < 1$. Hence, as expected, we are left with a single hump located at the correct position. This agrees with the $0 < \theta < 1$ case. In figures 5(*c*) and (*d*), we have drawn the function $|\langle b|\hat{B}|a\rangle|^2$ and its semi-classical approximation (103), respectively, when $a = \frac{3}{4} + \mathrm{i}/20$, $r = 2$ and $N = 8$. For such a large

dimension, $D = 2^8$, our semi-classical approximation becomes almost identical to the exact matrix element. One may also view our semi-classical propagator as an approximation to the Husimi function for the mapped state $\hat{B}|a\rangle$.

4. Conclusion

In this paper, we have derived the semi-classical form of the Schack–Caves quantum baker's maps, taking into consideration the different possible ways of obtaining the classical limit. We have shown that whenever the number of momentum bits becomes infinite in the limit $\hbar \to 0$, the quantum propagator in the coherent-state basis takes the Van Vleck form (51). Therefore, we conclude that the classical baker's transformation is restored for all such cases. In the case where the number of momentum bits is held constant, the classical limit is not that of the baker's transformation, but a stochastic variant. It may be possible one day to explore this discrepancy experimentally with the help of a quantum computer [7, 8]. As a final note, we remark that although our semi-classical formula (51) espouses a certain familiarity, we should not be presumptuous about its generality. One should, in general, expect extra phases in the exponent (see Baranger *et al* [41]). This has already been found in a spherical geometry for the case of the kicked top [11].

Acknowledgments

The authors would like to thank Carlton Caves for many helpful discussions and encouragement. This work was supported in part by the Office of Naval Research grant no N00014-00-1-0578.

References

[1] Lichtenberg A J and Lieberman M A 1992 *Regular and Chaotic Dynamics* (New York: Springer)
[2] Balazs N L and Voros A 1989 *Ann. Phys., NY* **190** 1
[3] Saraceno M 1990 *Ann. Phys., NY* **199** 37
[4] Hannay J H, Keating J P and Ozorio de Almeida A M 1994 *Nonlinearity* **7** 1327
[5] Rubin R and Salwen N 1998 *Ann. Phys., NY* **269** 159
[6] Lesniewski A, Rubin R and Salwen N 1998 *J. Math. Phys.* **39** 1835
[7] Schack R 1998 *Phys. Rev.* A **57** 1634
[8] Brun T A and Schack R 1999 *Phys. Rev.* A **59** 2649
[9] Pakoński P, Ostruszka A and Życzkowski K 1999 *Nonlinearity* **12** 269
[10] Schack R and Caves C M 2000 *Appl. Algebra Eng. Commun. Comput.* **10** 305
[11] Kuś M, Haake F and Eckhardt B 1993 *Z. Phys.* B **92** 221
[12] Scott A J and Milburn G J 2001 *J. Phys. A: Math. Gen.* **34** 7541
[13] Van Vleck J H 1928 *Proc. Natl Acad. Sci. USA* **14** 178
[14] Gutzwiller M C 1967 *J. Math. Phys.* **8** 1979
[15] Feynman R P and Hibbs A R 1964 *Quantum Mechanics and Path Integrals* (New York: McGraw-Hill)
[16] Brack M and Bhaduri R K 1997 *Semiclassical Physics* (Reading, MA: Addison-Wesley)
[17] Ozorio de Almeida A M and Saraceno M 1991 *Ann. Phys., NY* **210** 1
[18] Eckhardt B and Haake F 1994 *J. Phys. A: Math. Gen.* **27** 4449
[19] Saraceno M and Voros A 1994 *Physica* D **79** 206
[20] Dittes F-M, Doron E and Smilansky U 1994 *Phys. Rev.* E **49** R963
[21] Lakshminarayan A 1995 *Ann. Phys., NY* **239** 272
[22] da Luz M G E and Ozorio de Almeida A M 1995 *Nonlinearity* **8** 43
[23] Kaplan L and Heller E J 1996 *Phys. Rev. Lett.* **76** 1453
[24] Toscano F, Vallejos R O and Saraceno M 1997 *Nonlinearity* **10** 965
[25] Tanner G 1999 *J. Phys. A: Math. Gen.* **32** 5071
[26] Inoue K, Ohya M and Volovich I V 2002 *J. Math. Phys.* **43** 734

[27] Zurek W H 1982 *Phys. Rev.* D **26** 1862
[28] Giulini *et al* 1996 *Decoherence and the Appearance of a Classical World in Quantum Theory* (New York: Springer)
[29] Habib S, Shizume K and Zurek W H 1998 *Phys. Rev. Lett.* **80** 4361
[30] Bhattacharya T, Habib S and Jacobs K 2000 *Phys. Rev. Lett.* **85** 4852
[31] Scott A J and Milburn G J 2001 *Phys. Rev.* A **63** 042101
[32] Soklakov A N and Schack R 2000 *Phys. Rev.* E **61** 5108
[33] Griffiths R 1984 *J. Stat. Phys.* **36** 219
[34] Omnès R 1988 *J. Stat. Phys.* **53** 893
[35] Gell-Mann M and Hartle J B 1993 *Phys. Rev.* D **47** 3345
[36] Chang S-J and Shi K-J 1985 *Phys. Rev. Lett.* **55** 269
[37] Leboeuf P and Voros A 1990 *J. Phys. A: Math. Gen.* **23** 1765
[38] Nonnenmacher S 1998 *PhD Thesis* Université Paris XI
[39] Akhiezer N I 1990 *Elements of the Theory of Elliptic Functions* (Providence, RI: American Mathematical Society)
[40] Wong R 1989 *Asymptotic Approximations of Integrals* (Boston, MA: Academic)
[41] Baranger M, de Aguiar M A M, Keck F, Korsch H J and Schellhaaß B 2001 *J. Phys. A: Math. Gen.* **34** 7227